Evaluating the Potential of Fluorinated Tyrosines as Spectroscopic Probes of Local Protein Environments: A UV Resonance Raman Study†

Philip J. Reid,* Christine Loftus, and Craig C. Beeson*

Box 351700, Department of Chemistry, University of Washington, Seattle, Washington 98195

Received April 8, 2002

ABSTRACT: Ultraviolet resonance Raman (UVRR) studies designed to test the utility of fluorinated tyrosines as spectroscopic probes of the local environment are presented. Specifically, resonance Raman spectra of 2-fluoro-L-tyrosine and 3-fluoro-L-tyrosine (3-Y_f) obtained with 229 nm excitation are reported. In contrast to the modest environmental dependence of the tyrosine resonance Raman spectrum, the spectrum of 3-Y_f is found to be extremely dependent on the hydrogen bonding strength of the surrounding environment. Preliminary ab initio studies suggest that this behavior is due to normal modes having dominant contributions from the C-OH and C-F internal coordinates. Hydrogen bonding to the solvent perturbs the internal coordinate energetics and/or couplings, thereby altering the character of the normal modes and the corresponding transition frequencies and/or intensities. In addition to the solvent studies, 3-Y_f is site specifically incorporated into the influenza hemagglutinin (HA) 100−107 peptide which binds to the Fv fragment of the 17/9 anti-HA(98−108) peptide antibody. These studies demonstrate that the spectrum of 3-Y_f can be monitored in the presence of native tyrosine. In summary, the studies presented here demonstrate that 3-Y_f holds exceptional promise as a probe of the protein environment.

The ability of vibrational spectroscopies to provide both structural and dynamical information about proteins with residue specific detail has been recognized for some time. In these techniques, vibrational transitions localized on individual residues or transitions corresponding to modes delocalized over numerous residues are monitored as a function of perturbation (ligand binding, pH jump, protein unfolding, etc.) to study structural evolution. Infrared (IR) absorption and Raman scattering techniques have been developed to monitor the structural dynamics of proteins, and many excellent reviews of these areas are available (*1*−*5*). Although recent advances have been made in the application of vibrational spectroscopic techniques to large biological systems, efforts to provide residue specific information have involved ultraviolet resonance Raman (UVRR) spectroscopy of the aromatic amino acids (tyrosine, tryptophan, and phenylalanine) (*6*−*26*). These residues are attractive targets for UVRR studies due to the presence of relatively accessible absorption bands in the ultraviolet providing the opportunity for resonant enhancement. It was recognized early on that the different locations of the chromophore absorption bands allow for selective enhancement of a given residue type. For example, 229 nm excitation has been shown to selectively enhance tyrosine scattering (*22*). In addition, the frequencies and intensities of specific Raman-active tyrosine and tryptophan vibrational modes are known to be sensitive to the environment. In tryptophan, the W_4 and W_6 modes show an increase in frequency with an increase in hydrogen-bonding strength (*15*). The frequency of the ν_{8b} mode of tyrosine has been demonstrated to undergo a subtle change in frequency with an alteration in intermolecular hydrogen bonding strength (*20*, *23*). In addition, the relative intensities of the "Fermi doublet" of tyrosine, two transitions located at 832 and 852 cm^{-1}, have been proposed to undergo a significant evolution in intensity with a change in local hydrophobicity (*27*). UVRR spectroscopy has also proven to be extremely versatile. For example, evolution in the Fermi doublet region of the tyrosine spectrum has been used to study assembly of Ff virions (*28*). The environmental sensitivity of the resonance Raman spectrum has been used to investigate protein structural evolution following CO dissociation from hemoglobin (*18*, *20*, *25*). Finally, the UVRR spectrum of tryptophan has been used to monitor conformational dynamics in tyrosine phosphatases (*29*).

Although UVRR spectroscopy has undergone significant development in the past two decades, there are two main issues that continue to limit the applicability of this technique: spectral overlap and spectral sensitivity. The issue of spectral overlap arises from the fact that all residues of a given type will contribute to the resonance Raman spectrum. Frequently, the single residue or handful of residues experiencing a perturbation-induced evolution in environment will demonstrate spectral changes that must be studied in the presence of scattering from other environmentally invariant residues. Furthermore, the "background" associated with the environmentally invariant residues is expected to increase with the size of the biological system of interest. Finally, many of the aromatic−amino acid transitions overlap to a significant extent such that assignment of a transition to a specific amino acid type is not always straightforward (*28*). With regard to spectral sensitivity, the studies outlined above have shown that environmentally induced changes in the

† P.J.R. is the recipient of an Alfred P. Sloan Fellowship and is a Cottrell Scholar of the Research Corp. This work was supported in part by NIH Grant 1R01 GM59746-01 (C.C.B.).

* To whom correspondence should be addressed. E-mail: preid@chem.washington.edu (P.J.R.) or beeson@chem.washington.edu (C.C.B.).

10.1021/bi0202676 CCC: $25.00
Published on Web 01/28/2003

Chart 1

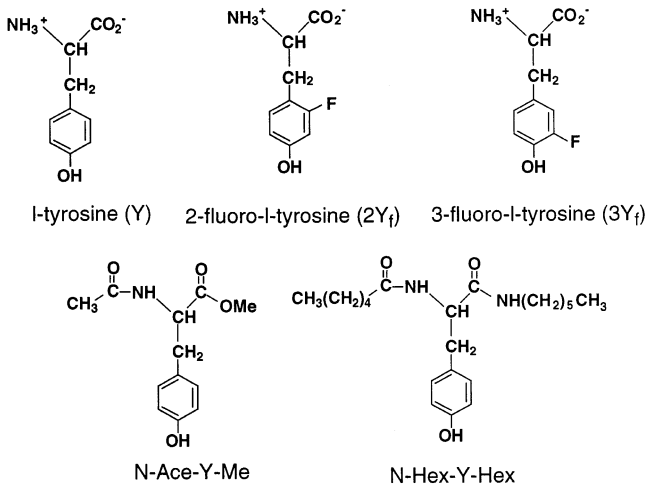

Raman spectrum can be extremely modest, placing severe demands on the signal-to-noise ratio necessary to monitor the spectral evolution of interest.

To address these limitations, we have initiated a series of studies in which non-natural amino acids are investigated as potential probes for UVRR studies of local protein environment. In particular, we are interested in developing and employing fluorinated analogues of the aromatic amino acids as such probes. Fluorinated amino acids have found wide application in ^{19}F NMR studies of protein structure and dynamics (*30*, *31*). The van der Waals radius of fluorine (1.35 Å) is similar to that of hydrogen (1.2 Å), so the steric perturbation introduced by fluorine substitution is minimal. In addition, biological functionality is generally maintained following the incorporation of fluorinated amino acids into proteins (*30*). Therefore, these probes provide a unique opportunity to further the application of UVRR in studies of protein structure while preserving biological functionality.

In this paper, we present a series of studies designed to ascertain the utility of fluorinated tyrosines as UVRR probes of local environment. The structures of tyrosine and its fluorinated analogues are presented in Chart 1. Using excitation at 229 nm, we report the first resonance Raman spectrum of 2-fluoro-L-tyrosine and 3-fluoro-L-tyrosine (3-Y_f). The spectrum of these residues is markedly different relative to that of native tyrosine, allowing for facile identification of the spectrum of the fluorinated residue. We present a series of experiments that compare the sensitivity of the tyrosine and 3-Y_f resonance Raman spectra to the local environment. Consistent with earlier studies, the resonance Raman spectrum of tyrosine is shown to demonstrate extremely subtle evolution as the hydrogen bonding strength of the solvent is modified. In contrast, dramatic evolution is observed for the 3-Y_f spectrum, demonstrating that this residue provides an extremely sensitive measure of the local environment. Finally, to test the utility of 3-Y_f in a biological system, we have site specifically incorporated this residue into the influenza hemagglutinin (HA) 100−107 peptide which binds to the Fv fragment of the 17/9 anti-HA(98−108) peptide antibody (*32*, *33*). The peptide spectra demonstrate that scattering from 3-Y_f can be isolated and studied in the presence of native tyrosine. In summary, the results presented here demonstrate that 3-Y_f holds great promise as a probe of local environment.

EXPERIMENTAL PROCEDURES

Resonance Raman Spectroscopy. The resonance Raman spectrometer used in these studies is described in detail elsewhere (*34*); therefore, only a brief description is presented here. Raman spectra were obtained with 229 nm excitation obtained from the hydrogen-shifted output from a 30 Hz Nd:YAG laser (Spectra Physics model GCR-170). The excitation light was weakly focused onto a flowing jet of the sample, and the flow rate was sufficient to sweep out the illuminated volume between laser shots. It has been recognized that one must employ modest excitation energies when acquiring resonance Raman spectra of aromatic amino acids to minimize photoalteration (*10*−*12*, *21*). Power-dependent studies were performed, and the observed intensities varied linearly with incident pulse energy under the conditions that were employed (10 μJ/pulse excitation). The scattered light was collected employing a back-scattering geometry using standard UV-quality refractive optics, and delivered to a 0.75 m spectrograph (Acton) coupled to a liquid nitrogen-cooled, back-illuminated CCD multichannel detector (Princeton Instruments). Holographic gratings with ruled densities of 3600 and 2400 g/mm were employed. Slit widths of 75 μm were employed providing for 4 cm^{-1} resolution. The reproducibility of transition frequencies was ±1 cm^{-1}.

Computational Studies. To assist in the assignment of the infrared and Raman transitions, a computational analysis designed to predict the normal coordinates of 2-fluoro-4-methylphenol, a model compound for 3-fluoro-L-tyrosine (3-Y_f), was performed. All calculations were performed using the Gaussian 98 program, revision A.7 (Gaussian, Inc.) (*35*). Both density functional theory (DFT) and Hartree−Fock (HF) methods were employed. The B3-LYP exchange correlation functional has been shown to accurately reproduce ground state vibrational frequencies; therefore, this functional was employed in the DFT calculations (*36*−*38*). Both DFT and HF calculations were initiated with the 6-31G* basis set. Typical computational times ranged from 6 to 15 h using DFT, and from 3 to 10 h using HF.

Materials. All reagents were obtained from Aldrich except for 2-fluoro-L-tyrosine (2-Y_f) and 3-Y_f, which were obtained from TCI (Portland, OR). L-Tyrosine (Aldrich 99.9% purity) was recrystallized twice before being used, and 2-Y_f and 3-Y_f (TCI) were used as received. All solvents that were employed were spectrophotometric grade. Phosphate-buffered saline (PBS, 150 mM NaCl and 10 mM sodium phosphate) was buffered to pH 7.4 and then filtered.

Synthesis of Functionalized Tyrosines. The *N*-acetyl-tyrosine methyl esters (*N*-Ace-Y-Me in Chart 1) were prepared by the addition of 2 equiv of acetic anhydride to a stirred solution of tyrosine or 3-Y_f in 1 M NaOH. After 10 min, a solution containing excess hydroxylamine was added to cleave any tyrosine phenoxyacetate. The residue obtained from an ethyl acetate extraction of the acidified reaction mixture was dissolved in methanol. An excess of diazomethane in ether was then added at 0 °C. The product, a waxy solid, was isolated using silica gel chromatography with 15% ethyl acetate in hexane. The *N*-hexanoyl-*N*-hexyl-tyrosine amides (*N*-Hex-Y-Hex in Chart 1) were prepared by the addition of 2 equiv of hexanoyl chloride to a stirred solution of tyrosine or 3-Y_f in 1 M NaOH. After 10 min, a solution containing excess hydroxylamine was added to

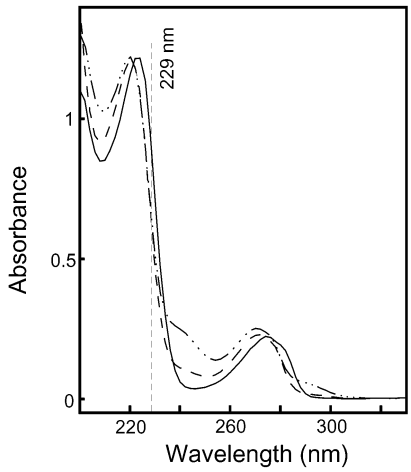

FIGURE 1: Electronic absorption spectra of L-tyrosine (—), 2-fluoro-L-tyrosine (– – –), and 3-fluoro-L-tyrosine (—···—) obtained in PBS buffer (pH 7.4). The spectrum of L-tyrosine is in agreement with previous studies (*22*). The excitation wavelength employed in this study (229 nm) is indicated.

cleave any tyrosine phenoxyhexanoate. The residue obtained from an ethyl acetate extraction of an acidified reaction mixture was dissolved in dimethylformamide, and a 4-fold excess of hexylamine, 1-hydroxybenzotriazole (HOBt), 2-(1*H*-benzotriazol-1-yl)-1,1,3,3-tetramethyluronium hexafluorophosphate (HBTU), and diisopropylethylamine (DIEA) were added. After 1 h, the reaction mixture was injected onto a preparative scale HPLC system (reverse phase, C18), and the product was isolated from an acetonitrile/water gradient.

Preparation of 2-Fluoro-4-methylphenol. In brief, 2-fluoro-5-methoxyaniline was treated with 1 equiv of sodium nitrite in a 48% fluoroboric acid solution at 0 °C. The diazonium fluoroborate salt that precipitated from the reaction mixture was thermally decomposed at 105 °C for 4 h, and the resulting 3-fluoro-4-methoxytoluene was isolated by silica gel chromatography (1:1 ether/hexane mixture). The methoxytoluene product was refluxed in concentrated HBr overnight, and the crude phenol obtained from an aqueous workup was purified by silica gel chromatography (ether). All compounds were characterized by electrospray mass spectrometry and ^{1}H NMR. The purity (≥95%) was assessed by analytical HPLC and ^{1}H NMR.

Preparation of a 3-Y_f-Labeled Peptide Fragment. The hemagglutinin 100−107 peptide (YDVPDY$_f$ AS) was synthesized on Rink amide resin using standard Fmoc chemistry (DIEA and HOBt/HBTU). After cleavage with 5% thioanisole in trifluoroacetic acid, the crude peptide was purified by reverse phase chromatography (C18, acetonitrile/water gradient). The Fmoc-3-fluorotyrosine was prepared by the reaction of 3-Y$_f$ with Fmoc-*N*-hydroxysuccinimide in a solution of 10% sodium bicarbonate (pH 8.5) for 48 h. The solution was filtered, acidified, and then extracted with ethyl acetate. The Fmoc-3-Y$_f$ was then isolated by silica gel chromatography (1:1 methanol/dichloromethane mixture).

RESULTS

Absorption Spectra. Figure 1 presents the electronic absorption spectrum of L-tyrosine (Y), 2-fluoro-L-tyrosine (2-Y$_f$), and 3-fluoro-L-tyrosine (3-Y$_f$). In the spectrum of Y, the L$_a$ (λ_{max} = 222 nm) and L$_b$ (λ_{max} = 275 nm) transitions

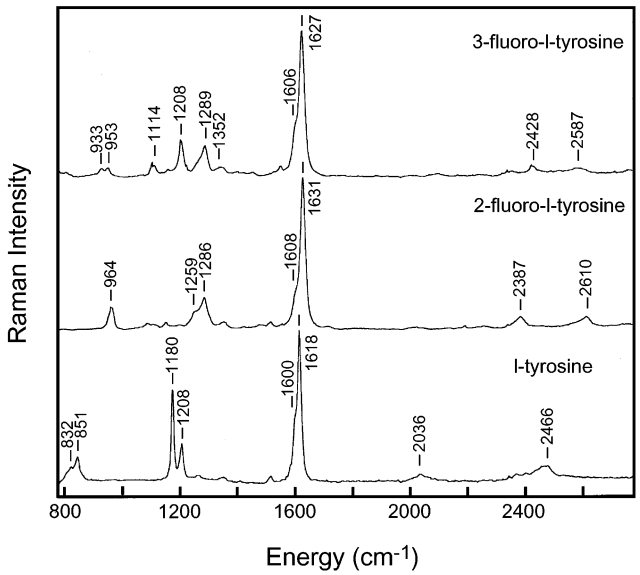

FIGURE 2: Resonance Raman spectra of 3-fluoro-L-tyrosine, 2-fluoro-L-tyrosine, and L-tyrosine dissolved in PBS buffer (pH 7.4). Spectra were obtained with 229 nm excitation.

are evident. The absorption spectra of the fluorinated derivatives are similar to that of Y, suggesting the character of the electronic transitions is not severely perturbed by fluorine substitution. However, subtle shifts in the absorption spectra are observed, with the maximum of the L$_a$ transitions decreasing to 219 ± 1 nm for both derivatives, and the maximum of the L$_b$ transitions decreasing to 273 ± 1 and 270 ± 1 nm for 2-Y$_f$ and 3-Y$_f$, respectively. In addition, the absorption intensity for 3-Y$_f$ between 235 and 260 nm has increased substantially relative to that of Y.

Resonance Raman Spectra. Figure 2 presents resonance Raman spectra of Y, 2-Y$_f$, and 3-Y$_f$ dissolved in PBS buffer (pH 7.4) obtained with 229 nm excitation. Since the fluorescence from these species occurs at wavelengths of >280 nm (*39*), the contribution of fluorescence to the background observed at this excitation wavelength is minimal. Figure 2 demonstrates that significant differences exist between the resonance Raman spectra of Y and the fluorinated analogues of Y. To address the origin of these differences, it is informative to start with the native chromophore itself. The pattern of intensities observed in the resonance Raman spectrum of L-tyrosine within the approximate C_{2v} symmetry of this chromophore has been extensively discussed (*10*, *11*, *22*). Excitation at 229 nm results in the enhancement of modes associated with the phenolic side chain of tyrosine. The 832 and 852 cm^{-1} modes, commonly termed the Fermi doublet, contain contributions from ring breathing (ν_1) and the overtone of an out-of-plane ring deformation mode ($2\nu_{16}$). The 1180 and 1208 cm^{-1} modes of Y are dominated by in-plane C−H bending and ring−C stretching, respectively. Finally, the transitions at 1600 (ν_{8a}) and 1618 cm^{-1} (ν_{8b}) are assigned to in-plane ring stretching. Accompanying fluorine substitution, the approximate symmetry of the chromophore and internal coordinate couplings are altered, resulting in a more complex pattern of scattered intensity. However, certain spectroscopic features reminiscent of Y remain intact for the fluorinated analogues. For example, both derivatives demonstrate intensity at ∼1600 cm^{-1} like the ν_{8a} and ν_{8b} transitions of Y. In addition, 3-Y$_f$ exhibits a doublet at 933 and 953 cm^{-1}

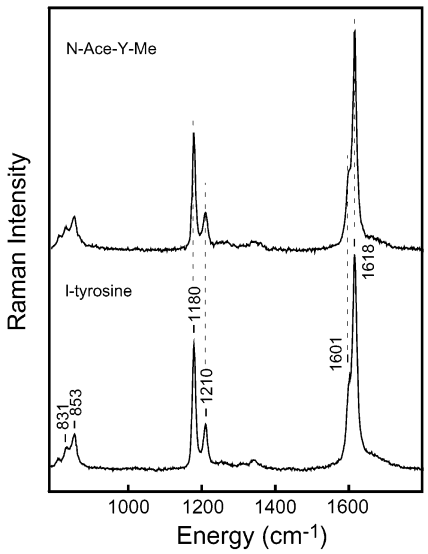

FIGURE 3: Resonance Raman spectra of native L-tyrosine and *N*-acetyltyrosine methyl ester (*N*-Ace-Y-Me), a functionalized tyrosine (Chart 1). The compounds were dissolved in PBS buffer (pH 7.4), and the spectra were acquired with 229 nm excitation. This figure demonstrates that the resonance Raman spectra are essentially identical such that functionalization has no apparent effect on the behavior of the phenolic side chain of L-tyrosine.

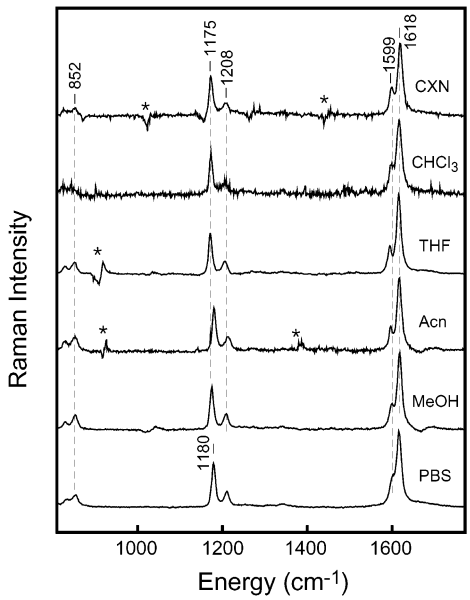

FIGURE 4: Solvent dependence of the resonance Raman spectra of native and functionalized tyrosines. Data were obtained with 229 nm excitation. Native tyrosine was investigated in PBS buffer and methanol (MeOH). The functionalized tyrosine *N*-Ace-Y-Me was investigated in PBS, methanol, acetonitrile (Acn), tetrahydrofuran (THF), and chloroform ($CHCl_3$). Finally, the spectrum of *N*-Hex-Y-Hex was obtained in acetonitrile, chloroform, and cyclohexane (CXN). Spectra for two different compounds in the same solvent were identical within the signal-to-noise ratio. This figure demonstrates that the resonance Raman spectrum of tyrosine obtained at this excitation wavelength is modestly sensitive to changes in the surrounding environment. Asterisks denote features arising from the subtraction of scattered intensity due to the solvent.

that resembles the Fermi resonance in the native chromophore. This assignment is supported by the existence of a Fermi doublet in *o*-methyl-substituted tyrosine (*27*). Assignments for other vibrational modes are discussed in detail below.

Solvent-Dependent Studies. The sensitivity of the Y resonance Raman spectrum to the environment has been investigated, and the frequency of the ν_{8b} mode has been demonstrated to correlate with the hydrogen bonding strength of the environment (*23*). Using *p*-cresol as a model for tyrosine, the frequency of the ν_{8b} mode was found to undergo a subtle decrease in frequency with an increase in hydrogen bonding strength in three aprotic solvents (acetone, diethyl ether, and triethylamine). In these studies, a change in the hydrogen bonding enthalpy of 5 kcal/mol was predicted to result in a relatively modest $\sim$4.5 cm^{-1} frequency shift of the ν_{8b} transition (*23*). In addition to this transition, the relative intensities of the Fermi doublet have also been observed to be sensitive to the environment. Specifically, the intensity ratio of this doublet, defined as I_{852}/I_{832}, changes from 10:4 in environments where the phenolic oxygen serves as a proton acceptor to 3:10 in environments where the phenolic hydroxyl group is a proton donor (*27*).

Use of *p*-cresol as a model compound was largely dictated by the enhanced solubility of this compound relative to that of Y. To investigate the environmental dependence of Y directly, we have synthesized a series of tyrosines in which the amine and carboxyl groups are functionalized, thereby increasing the solubility of Y in nonpolar solvents. Depictions of the functionalized tyrosines are presented in Chart 1. Figure 3 presents a resonance Raman spectrum of Y, and the functionalized tyrosine *N*-Ace-Y-Me in PBS buffer (pH 7.4) obtained with 229 nm excitation. The figure demonstrates that functionalization does not affect the pattern of intensities observed in the resonance Raman spectrum at this excitation wavelength. Since modes associated with the phenolic side chain of tyrosine dominate the resonance Raman spectrum at this excitation wavelength, invariance of the spectrum to functionalization is anticipated. Therefore, this control experiment demonstrates that the properties of the phenolic group are indeed unaltered with functionalization.

The environmental dependence of the Y resonance Raman spectrum as well as the spectrum of the functionalized tyrosines was determined by obtaining the spectra of these compounds in a variety of solvents as presented in Figure 4. Specifically, spectra were obtained in PBS for Y and *N*-Ace-Y-Me, in methanol for Y and *N*-Ace-Y-Me, in acetonitrile for *N*-Ace-Y-Me and *N*-Hex-Y-Hex, in tetrahydrofuran for *N*-Ac-Y-Me, in chloroform for *N*-Hex-Y-Hex, and in cyclohexane for *N*-Hex-Y-Hex. The variation in the signal-to-noise ratio between the spectra presented in Figure 4 is due to differences in concentration resulting from variations in solubility. No spectral differences were observed for any two species in the same solvent. The figure demonstrates that only very subtle changes are observed in the resonance Raman spectrum of Y as the solvent environment is varied. In the ν_{8a}/ν_{8b} region of the spectrum, both modes undergo a slight decrease in frequency from PBS to the aprotic hydrogen bond-accepting acetonitrile and tetrahydrofuran. In addition, the frequencies of the ν_{8a}/ν_{8b} transitions undergo an increase in frequency in cyclohexane relative to the frequencies in these aprotic solvents. Subtle changes are also observed for the 1180 cm^{-1} transition, with this mode undergoing a 5 ± 1 cm^{-1} downshift between PBS and cyclohexane. This observation is similar to the behavior observed for the corresponding transition in *p*-cresol (*14*).

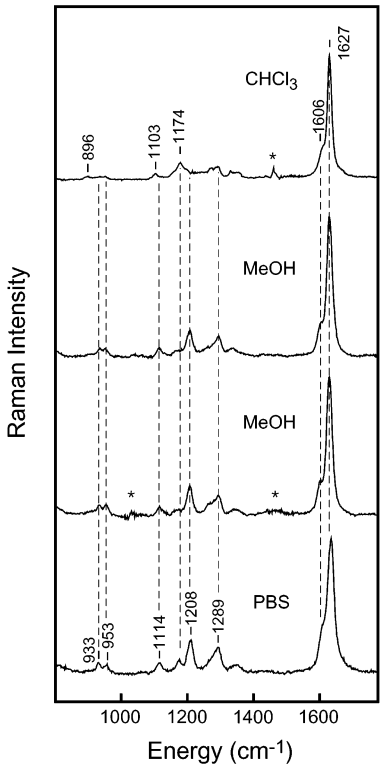

FIGURE 5: UV resonance Raman spectra of 3-fluoro-L-tyrosine and *N*-acetyl-3-fluorotyrosine methyl ester in various solvents. Spectra were obtained employing 229 nm excitation. The spectra in PBS buffer (pH 7.4) and the lower methanol (MeOH) spectra are those of 3-fluoro-L-tyrosine. The upper MeOH spectrum and the spectrum in chloroform ($CHCl_3$) are those of *N*-acetyl-3-fluorotyrosine methyl ester. The two MeOH spectra are essentially identical, demonstrating that functionalization of the amino termini of the chromophore does not affect the phenolic chromophore. Note that a dramatic evolution in the spectrum is observed when the hydrogen bonding strength of the solvent is varied. Asterisks denote features arising from the subtraction of scattered intensity due to the solvent.

Slight evolution is also observed in the Fermi doublet region of the spectrum. One concern in studying the functionalized tyrosines in nonpolar solvents is that the apparent paucity of the spectrum to changes in environment might arise from dimerization of the phenolic chromophores rendering the hydroxyl groups solvent inaccessible. To check this possibility, we performed FTIR and NMR studies in which transitions associated with the phenolic hydroxy group were monitored as a function of concentration. Through these studies, it was determined that any dimerization occurs through the amide functionality exclusively, and that dimerization of the phenolic groups does not occur at the concentrations investigated here. Therefore, the paucity of the Y resonance Raman spectrum to changes in environment is indeed characteristic of the chromophore.

In contrast to the spectrum of Y, the UVRR spectrum of 3-Y_f demonstrates substantial environmental dependence. Figure 5 presents resonance Raman spectra of 3-Y_f in PBS and methanol, and spectra of *N*-Ace-Y_f-Me dissolved in methanol and chloroform. The nomenclature used here is identical to that employed for tyrosine; however, Y is replaced with Y_f to indicate fluorine substitution. Two spectra in methanol are presented in Figure 5; the lower one corresponds to unfunctionalized Y_f and the upper one to the functionalized compound. The figure demonstrates that, like that of Y, the spectra of 3-Y_f and *N*-Ace-Y_f-Me are identical.

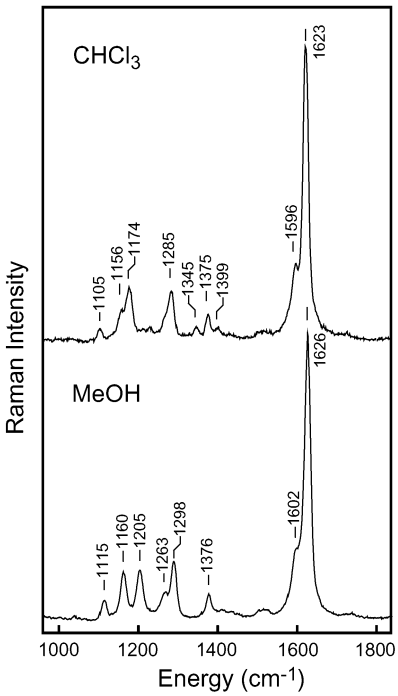

FIGURE 6: Resonance Raman spectra of 2-fluoro-4-methylphenol dissolved in chloroform (top) and methanol (bottom). Spectra were obtained with 229 nm excitation. Note that the evolution in the spectrum is remarkably similar to that observed for 3-fluorotyrosine.

Comparison of the PBS and methanol spectra demonstrates that the evolution in the spectrum is subtle, with the intensity of the 1289 cm^{-1} mode undergoing a slight decrease. However, when 3-Y_f is dissolved in chloroform, where the enthalpy for intermolecular hydrogen bonding is substantially decreased relative to that in PBS or methanol, the resonance Raman spectrum undergoes a dramatic change. The modes at 1208 and 1289 cm^{-1} have undergone a substantial decrease in intensity, and the strongest transition in the fingerprint region of the spectrum is now at 1174 cm^{-1}. In addition, the doublet at 933 and 953 cm^{-1} is reduced in intensity relative to the ν_{8a} transition, and the 933 cm^{-1} mode has undergone an apparent downshift to 896 cm^{-1}. Finally, the frequency of the 1114 cm^{-1} transition in PBS decreases to 1103 cm^{-1} in chloroform.

The results presented above demonstrate that the resonance Raman spectrum of 3-Y_f is remarkably sensitive to changes in the local environment. However, the question of why this should be the case remains. In particular, what is the internal coordinate composition of the normal modes whose transitions are sensitive to the environment? To address this question, an experimental and computational study was performed in which resonance Raman and infrared absorption spectra of 2-fluoro-4-methylphenol (2FMP), a model for 3-Y_f, were obtained and compared to the prediction of density functional theory (DFT) employing the B3-LYP exchange correlation functional. First, to ensure that 2FMP demonstrates the same sensitivity to environment as 3-Y_f, the resonance Raman spectrum of this compound dissolved in methanol and chloroform was obtained. Figure 6 presents the solvent dependence of the 2FMP resonance Raman spectrum, and demonstrates that the spectral evolution observed for this compound is similar to that observed for 3-Y_f. For example, in methanol a transition is evident at 1298 cm^{-1}, whereas a prominent transition at 1174 cm^{-1} is

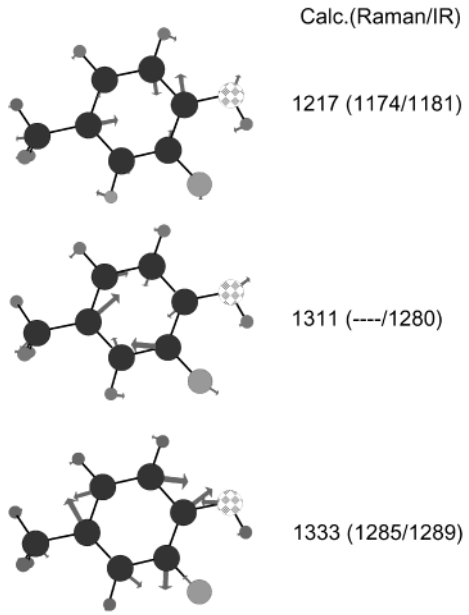

FIGURE 7: Depictions of three normal modes for which the corresponding transitions demonstrate sensitivity to solvent hydrogen bonding strength. The computation results were obtained using density functional theory as described in the text. The frequencies that are provided correspond to the unscaled computational frequencies, and in parentheses, the experimentally determined resonance Raman and IR frequencies are given.

observed in chloroform. We have developed preliminary normal mode descriptions for 2FMP transitions that demonstrate substantial sensitivity to environment, and depictions of these modes are presented in Figure 7. The calculations were performed on 2FMP in the absence of hydrogen bonding; therefore, the data obtained in chloroform (Figure 6) represent the best point for comparison. The figure presents the calculated mode frequencies (unscaled) and the frequencies observed in the resonance Raman and IR studies. The figure demonstrates that the transitions of interest contain significant internal coordinate contributions from the C−O stretch, the C−F stretch, and the C−O−H bend. Given these internal coordinate contributions, it is reasonable that hydrogen bonding involving the hydroxyl group of the phenolic chromophore or fluorine will significantly alter the character of the normal modes, with this effect reflected in an evolution in the resonance Raman spectrum. Further computational studies exploring the effect of intermolecular hydrogen bonding on the normal mode character of 2MFP are currently underway.

Discrimination between Y and 3-Y_f. As mentioned earlier, the two factors limiting the application of vibrational spectroscopy to problems in protein structure and dynamics are spectral overlap and spectral sensitivity. The results presented thus far demonstrate that the resonance Raman spectrum of 3-Y_f is highly dependent on environment, and that this compound provides an ideal opportunity to overcome limitations due to spectral sensitivity. With regard to spectral overlap, 229 nm excitation results in the preferential enhancement of tyrosine scattering; therefore, we anticipate endogenous tyrosine to be most problematic with respect to spectral overlap (*22*). To test the ability to differentiate 3-Y_f and Y scattering, 3-Y_f was substituted for one of two native tyrosines in the influenza hemagglutinin (HA) 100−107 peptide which binds to the 17/9 anti-HA(98−108)

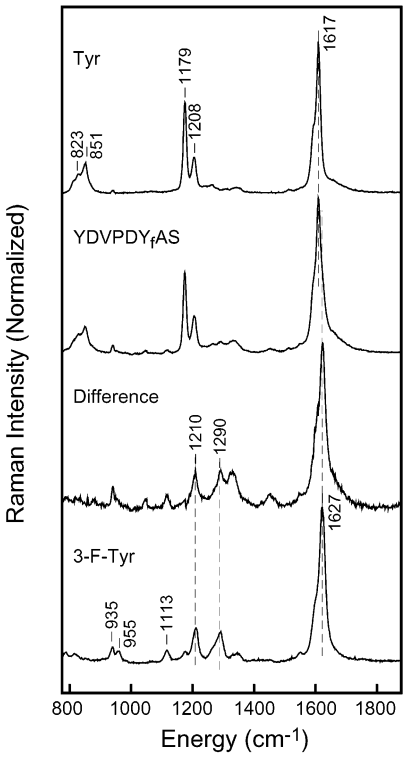

FIGURE 8: Resonance Raman spectra of the 100−107 peptide which binds to the Fv fragment of the 17/9 anti-HA(98−108) peptide antibody dissolved in PBS buffer (pH 7.4) obtained with 229 nm excitation. The peptide sequence is YDVPDY$_f$AS, where the subscript indicates the incorporation site of 3-fluoro-L-tyrosine (3-Y_f). Also presented in the figure are the corresponding spectra for L-tyrosine and 3-Y_f. Finally, the difference spectrum represents the difference between the peptide spectrum and the L-tyrosine spectrum. The difference spectrum is dominated by scattering due to 3-Y_f, demonstrating the ability to isolate scattering from the fluorinated residue even in the presence of endogenous tyrosine.

peptide antibody (*32*, *33*). The specific peptide sequence is YDVPDY$_f$AS, where the subscript indicates the 3-Y_f incorporation site. Figure 8 presents the resonance Raman spectrum of the fragment dissolved in PBS obtained with 229 nm excitation. Also presented are the resonance Raman spectra of Y and 3-Y_f . The figure demonstrates that the observed scattering is clearly dominated by Y and 3-Y_f. The difference spectrum presented in Figure 8 was obtained through subtraction of the Y spectrum from that of the peptide. The difference spectrum is essentially identical to that of 3-Y_f, with minor contributions arising from nonaromatic amino acids.

To determine the limit at which scattering assignable to 3-Y_f can be isolated in the presence of endogenous Y, mixtures of 3-Y_f and Y were studied (Figure 9). With 229 nm excitation, scattering from Y will make the dominant contribution to the resonance Raman spectrum of a protein (*22*); therefore, differentiating the scattering of 3-Y_f from Y will prove to be the limiting factor in the application of 3-Y_f in protein studies. Figure 9A presents the spectrum of a 2:1 molar mixture of Y and 3-Y_f. The spectrum demonstrates that indeed scattering from Y dominates the observed scattering. However, the difference between the spectrum of the 2:1 mixture and a spectrum of native tyrosine (Figure 9B) demonstrates that through subtraction of Y scattering, the resonance Raman spectrum of 3-Y_f can be retrieved. Figure 9C presents a spectrum of a 6:1 molar mixture of Y

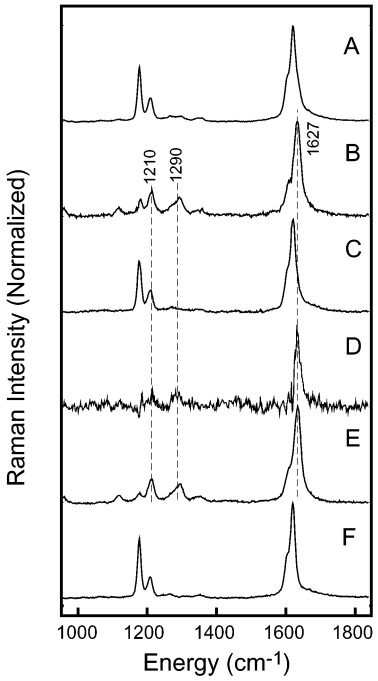

FIGURE 9: (A) Resonance Raman spectrum of a 2:1 molar mixture of Y and 3-Y_f obtained with 229 nm excitation. (B) Difference between the 2:1 spectrum and a spectrum of Y only. The difference spectrum is essentially identical to the resonance Raman spectrum of 3-Y_f. (C) Spectrum of a 6:1 molar mixture of Y and 3-Y_f. (D) Difference between the 6:1 spectrum and a spectrum of Y only. Resonance Raman spectra of Y (E) and 3-Y_f (F) are provided for comparison.

and 3-Y_f, and the corresponding difference spectrum is presented in Figure 9D. Inspection of this figure demonstrates that scattering from 3-Y_f is still evident. However, the signal-to-noise ratio is now roughly 2:1 such that this study provides a limiting case with respect to the concentration differential at which 3-Y_f scattering can be isolated. The data presented in parts C and D of Figure 9 correspond to a total acquisition time of 80 min; therefore, it is possible to employ a longer acquisition time in studies where more than six Y residues are present.

DISCUSSION

The results presented above demonstrate that 3-fluorotyrosine (3-Y_f) is an excellent probe of the local environment, and holds great promise as a UVRR probe for use in protein studies. As discussed above, the two central issues with respect to such probes are spectral overlap and spectral sensitivity. With regard to spectral overlap, the results presented above clearly demonstrate that fluorine substitution results in substantial differences between the resonance Raman spectra of 3-Y_f and tyrosine (Y). Therefore, transitions corresponding to 3-Y_f are readily observed even in the presence of Y. In addition, the results presented on the labeled HA peptide demonstrate that the paucity of the Y spectrum to changes in environment allows for facile subtraction of the Y resonance Raman spectrum such that the spectrum of 3-Y_f can be further isolated. Therefore, the combination of resonance enhancement and the unique spectra features of 3-Y_f relative to those of Y allow one to easily monitor the resonance Raman spectrum of this non-natural amino acid such that issues associated with spectral overlap are minimized.

With respect to spectral sensitivity, the results presented here clearly demonstrate that the resonance Raman spectrum of 3-Y_f obtained with 229 nm excitation demonstrates increased solvent sensitivity relative to Y. In agreement with earlier studies, the evolution of the Y spectrum as a function of solvent hydrogen bonding strength was found to be extremely modest. However, fluorine substitution gives rise to transitions for which the corresponding normal coordinates are remarkably sensitive to environment. From a phenomenological standpoint, the UVRR spectrum of 3-Y_f provides an elegant method by which to monitor changes in the environment experienced by this residue. However, what remains unclear is why the spectrum of 3-Y_f should be so sensitive to environment. One hypothesis for this behavior is provided by computational results outlined above. Specifically, the environmentally sensitive normal modes are predicted to contain substantial contributions from the C−O stretch, the C−F stretch, and the C−O−H bend internal coordinates. Given the similarity in mass between the F and OH groups, the internal C−F and C−O(H) stretch coordinates are expected to be similar in frequency; therefore, we would expect these coordinates to strongly couple. With the advent of hydrogen bonding, the effective mass of the OH and/or F groups will be altered, and the strength of the C−O and C−F bonds will be modified. As such, we would expect the coupling between the relevant internal coordinates to be altered, thereby affecting both the character and energetics of the normal modes depicted in Figure 7. In other words, the environmental sensitivity of 3-Y_f arises from an evolution in internal coordinate couplings and correspondingly the character of the normal modes. We are exploring this hypothesis through a series of computational studies in which the strength of hydrogen bonding to solvent will be systematically modified, and the character of the normal coordinates as a function of bonding strength will be studied.

ACKNOWLEDGMENT

We thank Josh McBee and James Chou for their contributions to this work.

REFERENCES

1. Thomas, G. J. J. (1999) *Annu. Rev. Biophys. Biomol. Struct. 28*, 1.
2. Callender, R. H., Dyer, R. B., Bilmanshin, R., and Woodruff, W. H. (1998) *Annu. Rev. Phys. Chem. 49*, 173.
3. Callender, R., and Deng, H. (1994) *Annu. Rev. Biophys. Struct. 23*, 215.
4. Ludlam, C. F. C., Arkin, I. T., Lui, X.-M., Rothman, M. S., Rath, P., Aimoto, S., Smith, S. O., Engelman, D. M., and Rothschild, K. J. (1996) *Biophys. J. 70*, 1728.
5. Braiman, M. S., and Rothschild, K. J. (1988) *Annu. Rev. Biophys. Biophys. Chem. 17*, 541.
6. Chi, Z., and Asher, S. A. (1998) *J. Phys. Chem. B 102*, 9595.
7. Chi, Z., and Asher, S. A. (1998) *Biochemistry 37*, 2865.
8. Sweeney, J. A., Harmon, P. A., Asher, S. A., Hutnik, C. M., and Szabo, A. G. (1991) *J. Am. Chem. Soc. 113*, 7531.
9. Larkin, P. J., Gustafson, W. G., and Asher, S. A. (1991) *J. Chem. Phys. 94*, 5324.
10. Teraoka, J., Harmon, P. A., and Asher, S. A. (1990) *J. Am. Chem. Soc. 112*, 2892.
11. Ludwig, M., and Asher, S. A. (1988) *J. Am. Chem. Soc. 110*, 1005.
12. Asher, S. A., Ludwig, M., and Johnson, C. R. (1986) *J. Am. Chem. Soc. 108*, 3186.
13. Harada, I., Yamagishi, T., Uchida, K., and Takeuchi, H. (1990) *J. Am. Chem. Soc. 112*, 2443.
14. Takeuchi, H., Watanabe, N., Satoh, Y., and Harada, I. (1989) *J. Raman Spectrosc. 20*, 233.

15. Harada, T., Takeuchi, H., and Harada, I. (1989) *J. Raman Spectrosc. 20*, 667.
16. Okishio, N., Fukuda, R., Nagai, M., Nagai, Y., Nagatomo, S., and Kitagawa, T. (1998) *J. Raman Spectrosc. 29*, 31.
17. Nagai, M., Imai, K., Kaminaka, S., Mizutani, Y., and Kitagawa, T. (1996) *J. Mol. Struct. 379*, 65.
18. Wang, D., Zhao, X., and Spiro, T. G. (2000) *J. Phys. Chem. A 104*, 4149.
19. Zhao, X., and Spiro, T. G. (1998) *J. Raman Spectrosc. 29*, 49.
20. Rodgers, K. R., Su, C., Subramaniam, S., and Spiro, T. G. (1992) *J. Am. Chem. Soc. 114*, 3697.
21. Su, C., Wang, Y., and Spiro, T. G. (1990) *J. Raman Spectrosc. 21*, 435.
22. Fodor, S. P. A., Copeland, R. A., Grygon, C. A., and Spiro, T. G. (1989) *J. Am. Chem. Soc. 111*, 5509.
23. Hildebrandt, P. G., Copeland, R. A., Spiro, T. G., Otlewski, J., Laskowski, M. J., and Prendergast, F. G. (1988) *Biochemistry 27*, 5426.
24. Copeland, R. A., and Spiro, T. G. (1985) *Biochemistry 24*, 4960.
25. Huang, S., Peterson, E. S., Ho, C., and Friedman, J. M. (1997) *Biochemistry 36*, 6197.
26. Huang, S., Huang, J., Kloek, A. P., Goldberg, D. E., and Friedman, J. M. (1996) *J. Biol. Chem. 271*, 958.
27. Siamwiza, M. N., Lord, R. C., and Chen, M. C. (1975) *Biochemistry 14*, 4870.
28. Overman, S. A., Aubrey, K. L., Vispo, N. S., Cesareni, G., and Thomas, G. J. J. (1994) *Biochemistry 33*, 1037.
29. Juszczak, L. J., Zhang, Z.-Y., Wu, L., Gottfried, D. S., and Eads, D. D. (1997) *Biochemistry 36*, 2227.
30. Danielson, M. A., and Falke, J. J. (1996) *Annu. Rev. Biophys. Biomol. Struct. 25*, 163.
31. Gerig, J. T. (1994) *Prog. Nucl. Magn. Reson. Spectrosc. 26*, 293.
32. Rini, J. M., Schultze-Gahmen, U., and Wilson, I. A. (1992) *Science 255*, 959.
33. Schulze-Gahmen, U., Rini, J. M., Arevalo, J., Stura, E. A., Kenten, J. H., and Wilson, I. A. (1988) *J. Biol. Chem. 263*, 17100.
34. Esposito, A., Foster, C., Beckman, R., and Reid, P. J. (1997) *J. Phys. Chem. A 101*, 5309.
35. Frisch, M. J., Trucks, G. W., Schlegel, H. B., Scuseria, G. E., Robb, M. A., Cheeseman, J. R., Zakrzewski, V. G., Montgomery, J. A., Jr., Stratmann, R. E., Burant, J. C., Dapprich, S., Millam, J. M., Daniels, A. D., Kudin, K. N., Strain, M. C., Farkas, O., Tomasi, J., Barone, V., Cossi, M., Cammi, R., Mennucci, B., Pomelli, C., Adamo, C., Clifford, S., Ochterski, J., Petersson, G. A., Ayala, P. Y., Cui, Q., Morokuma, K., Malick, D. K., Rabuck, A. D., Raghavachari, K., Foresman, J. B., Cioslowski, J., Ortiz, J. V., Stefanov, B. B., Liu, G., Liashenko, A., Piskorz, P., Komaromi, I., Gomperts, R., Martin, R. L., Fox, D. J., Keith, T., Al-Laham, M. A., Peng, C. Y., Nanayakkara, A., Gonzalez, C., Challacombe, M., Gill, P. M. W., Johnson, B. G., Chen, W., Wong, M. W., Andres, J. L., Head-Gordon, M., Replogle, E. S., and Pople, J. A. (1998) *Gaussian 98*, Gaussian, Inc., Pittsburgh, PA.
36. Rauhut, G., and Pulay, P. (1995) *J. Phys. Chem. 99*, 3093.
37. Scott, A. P., and Radom, L. (1996) *J. Phys. Chem. 100*, 16502.
38. Schettino, V., Gervasio, F. L., Cardini, G., and Salvi, P. R. (1999) *J. Chem. Phys. 110*, 3241.
39. Cantor, C. A., and Schimmel, P. R. (1980) *Biophysical Chemistry. Part II*: *Techniques for the Study of Biological Structure and Function*, W. H. Freeman and Co., New York.

BI0202676